

A RUN SCENARIO FOR THE LINEAR COLLIDER

PAUL D. GRANNIS

*Department of Physics and Astronomy, State University of New York,
Stony Brook NY 11790, USA*

We outline a run plan and examine the precision with which supersymmetric and Higgs parameters may be determined in 1000 fb^{-1} of running at the nominal 500 GeV e^+e^- linear collider, assuming the Snowmass benchmark mSUGRA point SM2 (similar to the SPS1 benchmark).

1 Introduction

The physics program of the linear e^+e^- collider (LC) can be very rich, particularly in the case that low mass supersymmetry exists. We examine a run plan for such a physics-rich case, in which the energies of the LC are selected to first measure the sparticle masses approximately using energy distributions at the highest available energy, followed by a series of scans at selected superparticle pair thresholds. In the supersymmetry part of this study, we pay attention to the way in which one can identify specific sparticle states based on the distinctive final states with little background. This paper is an update and extension of the study reported in the 2001 Snowmass Workshop proceedings¹.

We assume a physics scenario in which supersymmetry is characterized by the minimal supergravity model corresponding to the Snowmass SM2 benchmark ($m_0 = 100 \text{ GeV}$, $m_{1/2} = 250 \text{ GeV}$, $\tan \beta = 10$, $A_0 = 0$, and $\text{sign} \mu = +$). This benchmark point has nearly the same sparticle mass and branching ratios as the subsequent SPS1a point². We take the lightest Higgs boson mass to be 120 GeV, and to have standard model (SM) properties.

We have considered the initial 1000 fb^{-1} of LC running at 500 GeV, expected to take roughly the first seven years of operation. For runs below 500 GeV, we assume the luminosity falls as $1/E$. We assume that the LC operates with either left- or right-handed electron polarization of 80% and assume no positron polarization. The proposed runs and associated polarization states are given in Table 1. When a run with left or right polarization is called for, we assume that about 90% of the data is taken with the specified polarization and about 10% with the other polarization. This run plan differs from that in Ref.[1] in that there is no dominantly right polarization run at 410 GeV, and there is added running at the Z boson mass.

Table 1: Run allocations for the SPS1 Minimal Sugra parameters.

Beams	Energy	Pol.	$\int \mathcal{L} dt$	$[\int \mathcal{L} dt]_{\text{equiv}}$	Comments
e^+e^-	500	L/R	335	335	Sit at top energy for sparticle masses
e^+e^-	M_Z	L/R	10	45	Calibrate with Z 's
e^+e^-	270	L/R	100	185	Scan $\tilde{\chi}_1^0 \tilde{\chi}_2^0$ threshold (L pol.) Scan $\tilde{\tau}_1 \tilde{\tau}_1$ threshold (R pol.)
e^+e^-	285	R	50	85	Scan $\tilde{\mu}_R^+ \tilde{\mu}_R^-$ threshold
e^+e^-	350	L/R	40	60	Scan $t\bar{t}$ threshold Scan $\tilde{e}_R \tilde{e}_L$ threshold (L & R pol.) Scan $\tilde{\chi}_1^+ \tilde{\chi}_1^-$ threshold (L pol.)
e^+e^-	410	L	60	75	Scan $\tilde{\tau}_2 \tilde{\tau}_2$ threshold Scan $\tilde{\mu}_L^+ \tilde{\mu}_L^-$ threshold
e^+e^-	580	L/R	90	120	Sit above $\tilde{\chi}_1^\pm \tilde{\chi}_2^\pm$ threshold for $\tilde{\chi}_2^\pm$ mass
e^-e^-	285	RR	10	95	Scan with e^-e^- collisions for \tilde{e}_R mass

2 Initial estimates of sparticle masses from end points

For the SM2 Susy benchmark, the sparticle masses and primary decay branching ratios are as given in Table 2. The h^0 , H^0 , A^0 and H^\pm masses are 113, 380, 379 and 388 GeV respectively. The spartners of the lighter quarks and the gluino have masses of about 530 and 595 GeV. The two top squark masses are 393 and 572 GeV.

Although many particles are accessible at 500 GeV, the states $\tilde{\tau}_1$, $\tilde{\tau}_2$, $\tilde{\chi}_2^0$, $\tilde{\chi}_1^\pm$ have dominant decays into τ final states. In addition, the sneutrinos have dominant wholly invisible decays. On the other hand, the $\tilde{\chi}_3^0$ has distinctive decays involving Z bosons. Such observations are indicative of the fact that the Susy spectra are likely to vary drastically as parameters are changed, and thus specific conclusions on the precisions obtainable for sparticle properties in one scenario should not be blindly translated to others.

The traditional ‘end point’ mass determinations^{3,4} seek the sharp edges in the energy distribution of a SM particle C in the two body sparticle decay $\tilde{A} \rightarrow \tilde{B}C$. Such sharp edges require that a given final state channel under observation be fed mainly by just one Susy reaction, and that the SM particle C be stable. Neither of these conditions hold for many of the channels involved in our benchmark Susy point. The second condition is of course not actually required, since any *known* kinematic distribution can be fit with a set of templates derived for a set of hypothesized masses, and the best mass

Table 2: Masses (in GeV) and dominant branching fractions for the SM2 benchmark.

	M	Final state	(BR(%))
\tilde{e}_R	143	$\tilde{\chi}_1^0 e$ (100)	
\tilde{e}_L	202	$\tilde{\chi}_1^0 e$ (45)	$\tilde{\chi}_1^\pm \nu_e$ (34)
$\tilde{\mu}_R$	143	$\tilde{\chi}_1^0 \mu$ (100)	$\tilde{\chi}_2^0 e$ (20)
$\tilde{\mu}_L$	202	$\tilde{\chi}_1^0 \mu$ (45)	$\tilde{\chi}_1^\pm \nu_\mu$ (34)
$\tilde{\tau}_1$	135	$\tilde{\chi}_1^0 \tau$ (100)	$\tilde{\chi}_2^0 \mu$ (20)
$\tilde{\tau}_2$	206	$\tilde{\chi}_1^0 \tau$ (49)	$\tilde{\chi}_1^- \nu_\tau$ (32)
$\tilde{\nu}_e$	186	$\tilde{\chi}_1^0 \nu_e$ (85)	$\tilde{\chi}_1^\pm e^\mp$ (11)
$\tilde{\nu}_\mu$	186	$\tilde{\chi}_1^0 \nu_\mu$ (85)	$\tilde{\chi}_1^\pm \mu^\mp$ (11)
$\tilde{\nu}_\tau$	185	$\tilde{\chi}_1^0 \nu_\tau$ (86)	$\tilde{\chi}_1^\pm \tau^\mp$ (10)
$\tilde{\chi}_1^0$	96	stable	
$\tilde{\chi}_2^0$	175	$\tilde{\tau}_1 \tau$ (83)	$\tilde{e}_R e$ (8)
$\tilde{\chi}_3^0$	343	$\tilde{\chi}_1^\pm W^\mp$ (59)	$\tilde{\chi}_2^0 Z$ (21)
$\tilde{\chi}_4^0$	364	$\tilde{\chi}_1^\pm W^\mp$ (52)	$\tilde{\nu}_\nu$ (17)
$\tilde{\chi}_1^\pm$	175	$\tilde{\tau}_1 \tau$ (97)	$\tilde{\chi}_1^0 q\bar{q}$ (2)
$\tilde{\chi}_2^\pm$	364	$\tilde{\chi}_2^0 W$ (29)	$\tilde{\chi}_1^\pm Z$ (24)
			$\tilde{\ell} \nu_\ell$ (18)
			$\tilde{\chi}_1^\pm h$ (15)
			$\tilde{\nu}_\ell \ell$ (8)

obtained from the fits. The problem of multiple reactions feeding a particular observed channel is more serious, and must be addressed in detail for any given Susy benchmark. We comment here on the likely ability to determine sparticle masses for the SM2 benchmark. Our estimates of mass precision have been guided by previous studies^{3,4}, and we scale errors according to the ratio of our event samples relative to these studies.

We restrict attention to channels in which there are only leptons and missing energy, for which standard model backgrounds should be of little importance. We have followed the full decay chains of those sparticle pair reactions accessible at 500 GeV, weighted by their production cross sections and decay branching ratios. The number of events contributed to all 2, 4 and 6 lepton final states from all reactions that feed the channel were tabulated for each initial electron polarization state. No SM backgrounds are assumed. We have looked for the channel/polarization combination in which the production of a specific Susy particle are most dominant; in some cases there is no wholly dominant channel, and we imagine that a set of coupled-channel studies will be needed to get several sparticle masses simultaneously. We discuss the specific sparticle template mass determinations in turn.

The $\tilde{\mu}_R$ and $\tilde{\mu}_L$ masses are simple to obtain. The final state $\mu^+ \mu^- \not{E}$ with

Table 3: Reactions feeding the $\tau\tau\cancel{E}$ final state and the expected number of events before acceptance and efficiency losses in 335 fb^{-1} .

Reaction	$N(e_L)$	$N(e_R)$
$\tilde{\chi}_1^+ \tilde{\chi}_1^-$	97,440	11,229
$\tilde{\chi}_1^0 \tilde{\chi}_2^0$	29,424	6,846
$\tilde{\tau}_1^+ \tilde{\tau}_1^-$	11,792	29,547
$\tilde{\tau}_2^+ \tilde{\tau}_2^-$ (via $\tilde{\chi}_1^0 \tau$)	5,716	2,027
$\tilde{e}_L^+ \tilde{e}_L^-$	3,905	625
$\tilde{\mu}_L^+ \tilde{\mu}_L^-$	1,395	428
$\tilde{\tau}_2^+ \tilde{\tau}_2^-$ (via $\tilde{\chi}_1^\pm \nu_\tau$)	1,004	356
$\tilde{\tau}_1^\pm \tilde{\tau}_2^\mp$	805	644
$\tilde{\chi}_1^0 \tilde{\chi}_3^0$	71	85

right e^- polarization has 95% of its contribution from $\tilde{\mu}_R^\pm \tilde{\mu}_R^\mp$ production, and the decay $\tilde{\mu}_R \rightarrow \tilde{\chi}_1^0 \mu$ decay determines both the $\tilde{\chi}_1^0$ and $\tilde{\mu}_R$ masses. The final state $\mu^\pm \tau^\mp \cancel{E}$ final state from left polarized electrons is 95% due to $\tilde{\mu}_L^\pm \tilde{\mu}_L^\mp$ production, with one $\tilde{\mu}_L$ decay to $\tilde{\chi}_1^0 \mu$ and the other $\tilde{\mu}_L$ to $\nu_\mu \tilde{\chi}_1^\pm \rightarrow \nu_\mu \nu_\tau \tau \tilde{\chi}_1^0$. The μ energy distribution gives $M(\tilde{\mu}_L)$ in this case.

The $e^+ e^- \cancel{E}$ final state is dominated by the production of $\tilde{e}_R^+ \tilde{e}_R^-$, $\tilde{e}_R^+ \tilde{e}_L^-$, $\tilde{e}_L^+ \tilde{e}_R^-$ and $\tilde{e}_L^+ \tilde{e}_L^-$. A Snowmass study⁴ has shown that through the double difference of the distributions for e^+ and e^- end points with L - and R -polarized electrons, the masses of \tilde{e}_R , \tilde{e}_L (and $\tilde{\chi}_1^0$) can be well determined.

In benchmark SM2, the $\tau^+ \tau^-$ final states comingle many production processes. Table 3 shows the number of events from various contributing reactions for both electron polarizations. The $\tilde{\chi}_1^\pm$, $\tilde{\chi}_2^0$, and $\tilde{\tau}_1$ are all large contributors, so their masses must be extracted together. There are however some added features that help disentangle the reactions. As shown in Fig. 1, for the $\tilde{\chi}_1^+ \tilde{\chi}_1^-$ and $\tilde{\tau}_1^+ \tilde{\tau}_1^-$, the two τ 's tend to be back to back, whereas for $\tilde{\chi}_1^0 \tilde{\chi}_2^0$, the two τ 's come from the same parent $\tilde{\chi}_2^0$ and tend to be more collinear.

For the three dominant reactions feeding the left-polarized $\tau\tau\cancel{E}$ channel, the sparticles involved in specifying the energy distributions are the well-measured $\tilde{\chi}_1^0$, \tilde{e} , and $\tilde{\mu}$, together with the $\tilde{\chi}_1^\pm$, $\tilde{\chi}_2^0$ and $\tilde{\tau}_1$ whose masses we want to estimate. The energy distributions of the one-prongs from τ decays are not box-like, but are as shown in Fig. 2. These distributions can be fit however for the unknown sparticle masses using templates. For example, with the available statistics in 335 fb^{-1} , we find that the statistical error on the $\tilde{\tau}_1$ mass is 0.22 GeV when fitting such templates (keeping the $\tilde{\chi}_1^\pm$ and $\tilde{\chi}_2^0$ masses fixed). In a real analysis, all three masses must of course be varied, but more

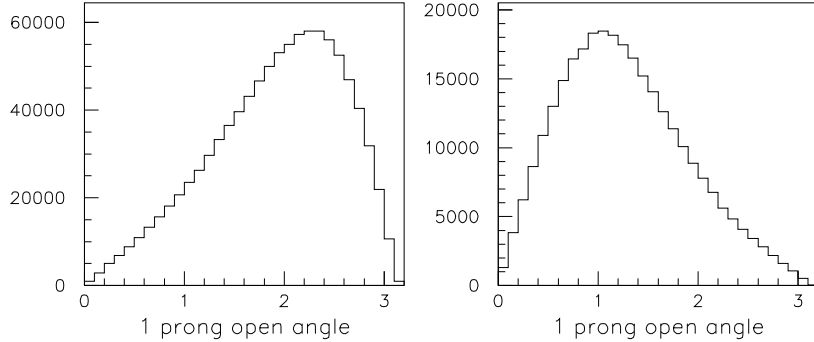


Figure 1: Opening angle of 1-prongs from τ decay (a) from reaction $\tilde{\chi}_1^+ \tilde{\chi}_1^-$ and (b) $\tilde{\chi}_1^0 \tilde{\chi}_2^0$ from left-polarized electrons.

channels may be employed.

Despite the fact that no single reaction dominates a particular channel, there are several channels that are dominated by the same unknown $\tilde{\chi}_1^\pm, \tilde{\chi}_2^0$ and $\tilde{\tau}_1$ masses in different proportions. For example the μ in the $\mu\tau\tau\tau$ channel with left polarization arises from $\tilde{\mu}_L \rightarrow \mu \tilde{\chi}_2^0$ 92% of the time (there are 1400 events before efficiency losses), so gives a reasonable determination of the $\tilde{\chi}_2^0$ mass. Other channels involving the same three sparticles are $\tau\tau$ (right polarized), $\mu\mu\tau\tau$ (left), $\mu\tau\tau\tau$ (left) and $\tau\tau\tau\tau$ (left). A careful study is needed to see how well the three unknown masses can be disentangled from a coupled channel analysis. I guess that precisions of about 1 GeV should be achievable from the 500 GeV runs, sufficient to locate the energy at which a scan should be performed.

The higher mass gaugino masses may be partly measurable. The $\tilde{\chi}_3^0$ has the useful and distinguishable decay modes, $\tilde{\chi}_3^0 \rightarrow \tilde{\chi}_1^0 (\tilde{\chi}_2^0) Z$ from which the $\tilde{\chi}_3^0$ mass can be determined, albeit with limited statistics. The $\tilde{\chi}_4^0$ mass though accessible kinematically, has event rates that are too small for a mass measurement. The $\tilde{\chi}_2^\pm \tilde{\chi}_1^\mp$ reaction threshold opens at 539 GeV in the SM2 benchmark; if we can deduce that this is likely to be the case, we would raise the LC energy to about 580 GeV to allow $\tilde{\chi}_2^\pm \tilde{\chi}_1^\mp$ production and give a rough estimate of the $\tilde{\chi}_2^\pm$ mass.

The $\tilde{\nu}$ masses are difficult to obtain in this scenario. The most favorable channel for isolating $\tilde{\nu}_e$ pair production is the $e\tau\tau\tau$ final state, where $\tilde{\nu}_e \tilde{\nu}_e^*$ contributes about 40% of the 6.5K events (before efficiency losses). The $ee\tau\tau$ and $e\mu\mu\tau$ channels have significant $\tilde{\nu}_e \tilde{\nu}_e^*$ contributions. Perhaps it is possible

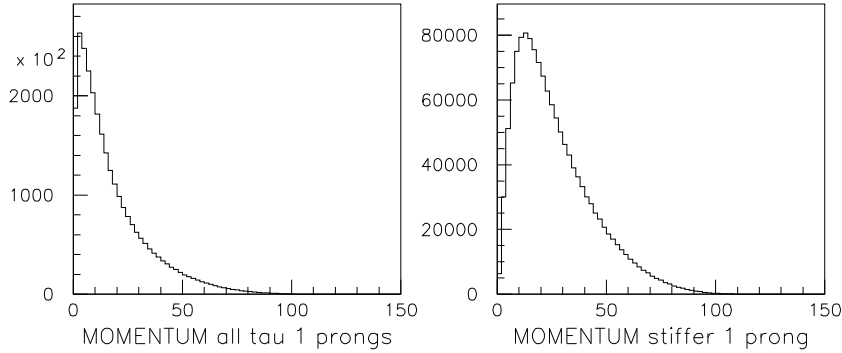


Figure 2: Energy distributions of 1-prongs from τ decay in the $\tau^+\tau^-$ channel; (a) all 1-prongs, and (b) the more energetic 1-prong.

to dig the $\tilde{\nu}_e$ mass out. The $\tilde{\nu}_\mu$ and $\tilde{\nu}_\tau$ seem hopeless to measure, as these sparticles do not come close to dominating any final state channel.

3 Sparticle threshold scans

Previous studies³ have examined the precision that can be attained on mass measurements from the appropriate energy scans near a two particle threshold. For this measurement, the problem of disentangling the reaction feeding a particular final state does not occur, providing that there are no overlapping thresholds in a particular channel. However, cross-sections near thresholds tend to be small, so the scans can use rather significant portions of the luminosity budget, and should be chosen for only those cases where there are substantial gains to be made.

The first studies³ of scans used ten energy points across the threshold in question. Subsequent studies^{5,6} have questioned this strategy, finding that particularly in the case of low $\sigma \times \text{BR}$ and relatively slow threshold turn-ons characteristic of sfermion pairs (β^3), fewer points on the scan may be better. An analytic study¹ that did not include the effects of backgrounds showed that the strategy for minimizing the errors shows little improvement for more than about three points on the scan.

One can improve the slope of the threshold curve for $\tilde{e}_R \tilde{e}_R$ by producing them in s -wave from an e^-e^- initial state (rather than in p -wave as for e^+e^-) even after the inclusion of beamsstrahlung effects and the reduced luminosity in e^-e^- operation⁷. We have adopted this strategy in our run plan.

Table 4: Mass precisions for the run plan of Table 1.

sparticle	δM end point	δM scan	δM combined
\tilde{e}_R	0.19	0.02	0.02
\tilde{e}_L	0.27	0.30	0.20
$\tilde{\mu}_R$	0.08	0.13	0.07
$\tilde{\mu}_L$	0.70	0.76	0.51
$\tilde{\tau}_1$	$\sim 1 - 2$	0.64	0.64
$\tilde{\tau}_2$	—	1.1	1.1
$\tilde{\nu}_e$	~ 1	—	~ 1
$\tilde{\nu}_\mu$	7?	—	7?
$\tilde{\nu}_\tau$	—	—	—
$\tilde{\chi}_1^0$	0.07	—	0.07
$\tilde{\chi}_2^0$	$\sim 1 - 2$	0.12	0.12
$\tilde{\chi}_3^0$	8.5	—	8.5
$\tilde{\chi}_4^0$	—	—	—
$\tilde{\chi}_1^\pm$	$\sim 1 - 2$	0.18	0.18
$\tilde{\chi}_2^\pm$	4	—	4

The estimated precisions were scaled from those of previous threshold scan studies. We have not explicitly included the effects arising from differences in background at our benchmark point relative to previous studies. However, we conservatively considered only the dominant channel and polarization state.

4 Susy mass and parameter precisions attainable

The mass precisions obtained for the run plan of Table 1 are shown in Table 4. Given these mass precisions and making the assumption that the supersymmetry is indeed mSUGRA, the errors that can be obtained for the Susy parameters are shown in Table 5.

5 Higgs and top quark studies

The Higgs production processes occur at most of the energies in our run plan; there as many ZH events over the full run as would be obtained in about 525 fb^{-1} of running at 350 GeV, or in about 1220 fb^{-1} at 500 GeV. We do not expect that running at several energies should materially affect the Higgs parameter determinations, and we simply scale the precision obtained in previous

Table 5: Errors on mSUGRA parameters.

parameter	SPS1
m_0	100 ± 0.08 GeV
$m_{1/2}$	250 ± 0.20 GeV
A_0	0 ± 13 GeV
$\tan \beta$	10 ± 0.47

studies^{8,9} by the statistics of the ZH sample. We have used the somewhat more favorable estimates for the TESLA study⁸, but note that there is still some uncertainty on the branching ratio errors, in particular for $c\bar{c}$ decays. The projected Higgs parameter errors are shown in Table 6. Use of Higgs bosons produced through WW fusion may improve the situation somewhat.

The top quark parameters are taken from the scan near the $t\bar{t}$ threshold at 350 GeV. The statistical errors are expected to be small compared with the theoretical errors associated with QCD theory. We may expect that the mass and width of the top quark may be determined to 150 MeV and about 70 MeV respectively in the 40 fb^{-1} allocated to this threshold. (Less luminosity would be needed to saturate expected theory errors for the top quark, but the $t\bar{t}$ threshold overlaps those of $\tilde{e}_L \tilde{e}_R$ and $\tilde{\chi}_1^+ \tilde{\chi}_1^-$, for which larger luminosity accumulations are desired.)

6 Calorimeter calibrations

It will be necessary to make good relative calibrations of the calorimeter energy scale in a LC detector, so as to capitalize upon the excellent intrinsic resolution of the calorimeter. These should be done with a periodicity that is shorter than the gain-drift time for the calorimeter. Two methods could be envisioned: the first employing special runs at the Z boson mass, and the second using data collected during ordinary running at higher energies.

Our run plan in Table 1 calls for four runs of 2 fb^{-1} each at the Z (every other year). Others would ask for more – perhaps one per year. For each such run, we expect 3.6 million $Z \rightarrow ee$ or $\mu\mu$ and 76 million $Z \rightarrow$ hadrons. We assume a calorimeter with of order 10^6 EM towers and 5×10^4 hadronic towers, and suppose that we calibrate 2×2 blocks of these as fundamental units. We take the calorimeter energy resolutions to be $\delta E/E = 0.15/\sqrt{E} \oplus 0.005$ (EM) and $\delta E/E = 0.4/\sqrt{E} \oplus 0.01$ (hadronic). Then we obtain about 28 electrons in each EM calibration block and about 24K hadrons in each hadronic block. In each block, the precision on the Z mass measurement is given by $\delta M =$

Table 6: Relative errors (in %) on Higgs mass, cross-section, total width, branching ratios and Yukawa couplings (λ) for the run plan of Table 1.

Parameter	error	Parameter	error
Mass	0.03	Γ_{tot}	7
$\sigma(ZH)$	3	λ_{ZZH}	1
$\sigma(WW)$	3	λ_{WWH}	1
$\text{BR}(b\bar{b})$	2	λ_{bbH}	2
$\text{BR}(c\bar{c})$	8	λ_{ccH}	4
$\text{BR}(\tau^+\tau^-)$	5	$\lambda_{\tau\tau H}$	2
$\text{BR}(gg)$	5	λ_{ttH}	30

σ_M/\sqrt{N} , with $\sigma_M/M \approx \delta E/E$ at $E = M_Z$. The resulting mass measurements for each block yield a statistical error on the Z mass, and hence a calibration accuracy of 0.38% (EM) and 0.03% (hadronic). Since these precisions are small compared with the intrinsic energy resolution smearing, they should be adequate for measurements of SM and Susy masses.

It is highly desirable to have calibration methods that can be performed during high energy running, and thus can track changes in calibration. Bhabha scattering has been studied as a means of continuous EM calibration. Here we focus on an alternate method using ‘energy flow’ (not to be confused with the technique of substituting charged particle momentum measurements for calorimeter energy deposits). We define energy flow to be the relative number of events seen above some arbitrary energy threshold, over a ring of cells at fixed azimuth. The azimuthal symmetry for physics processes means that observed variations are due to differences in the relative gain constants α_i for the set of cells in the ring ($E_{\text{true}} = \alpha E_{\text{meas}}$). A simplified estimate of the calibration precision obtainable can be made assuming that the energy spectrum in a given azimuthal ring is given by $dN/dE = Ae^{-BE}$. Then for N events above an energy threshold E_{th} , one can show that $\delta\alpha = 1/(BE_{\text{th}}\sqrt{N})$, and the optimum (smallest $\delta\alpha$) choice of threshold is $E_{\text{th}} = 2/B$.

For 10 fb^{-1} of data at 500 GeV and the inclusive particle spectrum (we actually used the flatter 1000 GeV Monte Carlo spectrum¹⁰, and hence conservative for our purposes), and with 200 cells at fixed ϕ for each of 20 bins in $\cos\theta$, we find that a 1% calibration can be obtained. Though of poorer precision than the special Z pole calibration, this is a very useful check for drifts in the calibration during high energy running. The method itself can be checked with energy flow measurements at the Z pole, where we estimate a precision of about 0.8% for each cell. Cross calibration of different azimuthal

Table 7: Profile by year of the luminosity accumulation. The luminosity is given in fb^{-1} assuming 500 GeV operation.

Year	1	2	3	4	5	6	7
$\int \mathcal{L} dt$	10	40	100	150	200	250	250

rings would be performed using Z bosons from the high energy runs.

The absolute energy calibration of the calorimeter at the 0.03% level is desired to match the expected statistical precision of the Higgs boson mass measurement. This can be obtained after relative calibration of the calorimeter blocks in the special Z pole runs discussed above, and should yield calibration of both EM and hadronic calorimeters to the requisite accuracy.

7 Run order

We should note that before the LC run plan is constructed, we will have an understanding of the actual physics scenario from the LHC/Tevatron. In particular, the Higgs mass will be known and the presence or absence of supersymmetry will be established. The run order given here assuming the SM2 Susy scenario discussed above is not well tuned, but is offered to guide our thinking. Clearly the initial stages will also be constrained by the progress of the accelerator complex. We assume the growth of luminosity in the LC to be that given in Table 7.

1. In the first year, if 500 GeV operation is feasible, it would be profitable to run there to get a first indication of the masses of the easier Susy particles to observe. In the 10 fb^{-1} , we expect $\sim 700 ZH$ events at 500 GeV. If 500 GeV running is not available, operation at 350 GeV would be called for ($\sim 1500 ZH$ events). If it is only possible to run at low energy, then one would devote the initial running to the Z pole.
2. Go to 500 GeV as soon as possible for $\sim 80 \text{ fb}^{-1}$ to obtain about two times the ultimate errors on sparticle masses. This should be sufficient to establish the $\tilde{e}_L, \tilde{e}_R, \tilde{\mu}_L, \tilde{\mu}_R$, and $\tilde{\chi}_1^0$ masses well, and give reasonable estimates for $\tilde{\chi}_2^0, \tilde{\chi}_1^\pm$, and $\tilde{\tau}_1$ masses.
3. Scans at 285 GeV ($\tilde{\mu}_L \tilde{\mu}_R$ threshold) and at 350 GeV ($t\bar{t}, \tilde{e}_L \tilde{e}_R$, and $\tilde{\chi}_1^+ \tilde{\chi}_1^-$ thresholds).
4. Complete the 500 GeV run for the ultimate precision on end point masses, and for disentangling the multi- τ final states.

5. Scan at 270 GeV ($\tilde{\chi}_1^0 \tilde{\chi}_2^0$ and $\tilde{\tau}_1 \tilde{\tau}_1$ thresholds).
6. Scan at 285 GeV using $e^- e^-$ initial state to give the precise \tilde{e}_R mass.
7. Operate at above the nominal top energy at 580 GeV with $e^+ e^-$ to do the $\tilde{\chi}_1^\pm \tilde{\chi}_2^\mp$ study and obtain the $\tilde{\chi}_2^\pm$ mass.

Note that no Giga-Z run is called for our SM2 Susy scenario, since the need to provide the extra Z -pole (and more precise W mass) is not so great in the scenarios where supersymmetry provides the mechanism for EWSB.

8 Considerations for a run scenario if it's not Susy

If the world we inhabit does not include low mass supersymmetry, we will know this at the start of the LC operation. In this world, there are two avenues for exploring the character of EWSB: observe new states or deviations in cross-sections from SM predictions at high energy; and improve our knowledge of the precision electroweak observables at the Z pole and WW threshold. The run plan in this case should reflect these two paths, and we outline such a plan below. Approximate equivalent luminosity acquisitions (the accumulations that would have occurred in the same time at 500 GeV) are given in parentheses. We have not specified the order in which the runs might be taken, but clearly those involving very careful understanding of the beam energies (for the WW threshold run), positron polarization (for Giga- Z), or $\gamma\gamma$ collisions should be left for later in the program when the machine is well-understood.

1. (500 fb^{-1}) Look for new high mass phenomena
2. (150 fb^{-1}) Run at the highest accessible energy by trading off luminosity for energy. Seek new signals at higher energies and new physics energy dependences.
3. (100 fb^{-1}) Obtain the full Giga- Z sample, with polarized e^+ . About 20 fb^{-1} are needed at the Z (thus $\mathcal{L}_{\text{equiv}} \approx 100 \text{ fb}^{-1}$).
4. (150 fb^{-1}) Run with $\gamma\gamma$ collisions at the maximum energy available to give an alternate view to $e^+ e^-$ collisions for the trilinear gauge couplings, heavy Z' , or complementary sensitivity to large extra dimensions.
5. (80 fb^{-1}) Scan the WW threshold for a precision W boson mass measurement.
6. (20 fb^{-1}) Scan the $t\bar{t}$ threshold for precision top quark mass and width information.

9 Conclusions

In the delightful case that Nature provides us with low mass supersymmetry, the LC should offer the possibility for extensive and precise measurements to point the way for understanding EWSB and the character of physics beyond the SM. The details of the run plan will depend critically upon the exact model that we encounter. Considerable ingenuity may be required to unscramble the effects of many accessible supersymmetric particles, but in the τ -rich case examined here, it seems possible to do a good job with this. Even for the low mass Susy situation studied here, much running at 500 GeV is needed to establish a good picture of the various sparticle masses. And it remains clear that further studies at energies above 500 GeV will be needed in this, or other conceivable physics scenarios.

Acknowledgments

I am grateful to G. Bernardi, G. Blair, J. Butler, R. Cahn, J.K. Mizukoshi, U. Nauenberg and G.W. Wilson for important contributions to the studies reported here. This work was supported by the US National Science Foundation, grant 0096707.

References

1. M. Battaglia *et al.*, Proceedings of Snowmass 2001, eConf C010630, SLAC-R-599, ed. Norman Graf, paper E3006 (hep-ph/0201177).
2. B.C. Allanach, hep-ph/0202233.
3. H.U. Martyn and G. Blair, hep-ph/9910416.
4. U. Nauenberg *et al.*, Proceedings of Snowmass 2001, eConf C010630, SLAC-R-599, ed. Norman Graf, paper E3056.
5. J.K. Mizukoshi, H. Baer, A.S. Belyaev, X. Tata, hep-ph/0107216.
6. G. Blair, Proceedings of Snowmass 2001, eConf C010630, SLAC-R-599, ed. Norman Graf, paper E3019.
7. J. Feng and M. Peskin, hep-ph/0105100.
8. “*TESLA Technical Design Report*”, DESY 2001-011, (March 2001), http://tesla.desy.de/new_pages/TDR_CD/start.html.
9. “*Linear Collider Physics Resource Book for Snowmass 2001*”, American Linear Collider Working Group, SLAC-R-570, <http://www.slac.stanford.edu/grp/th/LCBook/>.
10. T. Barklow, private communication.